ADVANCED MATERIALS
www.advmat.de

Check for updates

Functional Materials Under Stress: In Situ TEM Observations of Structural Evolution

Yu Deng, Ruopeng Zhang, Thomas C. Pekin, Christoph Gammer, Jim Ciston, Peter Ercius, Colin Ophus, Karen Bustillo, Chengyu Song, Shiteng Zhao, Hua Guo, Yunlei Zhao, Hongliang Dong, Zhiqiang Chen, and Andrew M. Minor*

The operating conditions of functional materials usually involve varying stress fields, resulting in structural changes, whether intentional or undesirable. Complex multiscale microstructures including defects, domains, and new phases, can be induced by mechanical loading in functional materials, providing fundamental insight into the deformation process of the involved materials. On the other hand, these microstructures, if induced in a controllable fashion, can be used to tune the functional properties or to enhance certain performance. In situ nanomechanical tests conducted in scanning/transmission electron microscopes (STEM/TEM) provide a critical tool for understanding the microstructural evolution in functional materials. Here, select results on a variety of functional material systems in the field are presented, with a brief introduction into some newly developed multichannel experimental capabilities to demonstrate the impact of these techniques.

Prof. Y. Deng, Y. Zhao
Solid State Microstructure National Key Lab and Collaborative Innovation Center of Advanced Microstructures
Nanjing University
Nanjing 210093, China
E-mail: dengyu@nju.edu.cn

R. Zhang, Dr. T. C. Pekin, Prof. J. Ciston, Prof. P. Ercius, Prof. C. Ophus, Dr. K. Bustillo, C. Song, Dr. S. Zhao, Prof. A. M. Minor
National Center of Electron Microscopy
Molecular Foundry
Lawrence Berkeley National Laboratory
Berkeley, CA 94720, USA

R. Zhang, Dr. T. C. Pekin, Dr. S. Zhao, Prof. A. M. Minor
Department of Materials Science and Engineering
University of California
Berkeley, CA 94720, USA

Prof. C. Gammer
Erich Schmid Institute of Materials Science
Austrian Academy of Sciences
Jahnstrasse 12, 8700 Leoben, Austria

Prof. H. Guo
Department of Materials Science and NanoEngineering
Rice University
Houston, TX 77251, USA

Dr. H. Dong, Prof. Z. Chen
Center for High Pressure Science and Technology Advanced Research
Shanghai 201203, China

The ORCID identification number(s) for the author(s) of this article can be found under https://doi.org/10.1002/adma.201906105.

DOI: 10.1002/adma.201906105

1. Introduction

The properties of functional materials are strongly determined by the underlying microstructure, which is usually sensitive to the operating conditions during specific applications. Observing and characterizing the dynamic process of the microstructure is therefore key to understanding the structure–property relationship.[1–7] It is also possible to tune the microstructure of a material by using electrical, magnetic, thermal, and stress fields, leading to significant property improvements.[8–17] Among them, high-stress load is proved to be an attractive and challenging one. Under very high pressure (stress), many unexpected amazing performances have been recently found out of the well-known materials, such as the very-high-temperature superconductive phase transition and metallic hydrogen under high stress.[18–20] Also, high stress can introduce extremely small microstructures into materials,[21–26] as well as cause complex across-scale local microstructure evolutions,[8,21,24,27–33] showing great potentials for novel functional micro-/nanodevice applications.

Therefore probing microstructure evolution and defect motion in functional materials under high stress is a topic of great interest, which is one of the best ways to reveal the mechanism of functional property tuning and material failure by mechanical loading. Encouragingly, the recent advances in in situ electron microscope has enabled us to perform real time probing on the complex microstructures, from atomic to micrometer scales under quantitatively loaded high stress.[34–40] With the new generation of aberration-corrected (scanning) transmission electron microscopes (STEM/TEM) that are equipped with a fast direct detect device (DDD) camera,[2,40] we are able to conduct atomic-resolution low-dose imaging[41] with unprecedented clarity. Features as small as interstitials, substitutional atoms, and even vacancies are visible in matters.[1,42,43] And real-time nanobeam electron diffraction (NBED) mapping in in situ STEM (also called 4D-STEM) is available,[40] where the read-out speed of TEM camera has been greatly improved by the developments of both fast DDD cameras and software for treatment of big data.[44–48] As known, for conventional postmortem TEM and STEM observations, various information is extracted by alternating the imaging conditions. Therefore in the case of in situ

 © 2019 WILEY-VCH Verlag GmbH & Co. KGaA, Weinheim

mechanical test, TEM observation is usually restrained to a certain imaging condition, leading to poor multiscale and multicontrast imaging of dynamical process. Now, 4D-STEM has the capability to monitor the complete local diffraction information with a spatial resolution down to a unit cell. More, as the fabrication of micro-electro-mechanical system (MEMS) devices comes to maturity, it has been widely integrated into in situ TEM to measure properties of functional materials which are under stress loads.[49–52] Many MEMS devices with built-in actuators and sensors have developed to locally conduct the on-chip tests.[53] It provides an extraordinary way to explore the relationship between the functional properties and the stress-induced local microstructures.

Herein, several examples of current progress regarding in situ mechanical TEM/STEM techniques have been addressed, which allow real-time probing of local microstructures (from atomic to micrometer scales) in functional materials that are under high stress loads. The advancements of these state-of-the-art techniques make it come true to study the materials behavior with unprecedented temporal and spatial resolution, yielding new insights into phenomena that are unable to be probed by conventional methods.

2. Probing of Functional Materials by Using In Situ Mechanical TEM

The in situ TEM/STEM observation during mechanical loading was originally used to study structural materials, such as the deformation behaviors and defect motions.[54–60] For example, the mechanical TEM holder with an actuation system, as well as the device made of two materials which have various thermal expansion coefficients, have been used to strain thin materials in in situ TEM.[34,61–63] Taking advantage of the accurate positioning capability of piezoelectric stacks and tubes, nanoindentation tip has been lately integrated into the in situ TEM, allowing not only accurate moving of the indenter, but also precision measuring of the load.[57–59,61,63,64] In addition, a variety of punch tips, sample stages, and in situ chips being mounted on the sample stages have been integrated into in situ nanomechanical system, to induce more and more functions.[65–69] Encouragingly, besides structural materials, many functional materials have also been well studied by the in situ mechanical TEM/STEM, showing the promising stress/strain-dependent functional properties.[70–72] Here, we describe a few examples of recent progress in in situ probing of local structure in functional materials under high stress/strain. The local structures from atomic to micrometer scales can be precisely probed in real time under the high stress of 0.1–1 GPa level. The stress level is strongly correlated with the mechanical-performance requirement of most functional materials. It is also widely used to introduce microstructure evolutions (e.g., phase transition and domain switching) in functional materials for the stress-dependent property tuning.[71,72]

2.1. In Situ Functionality Measurement under Mechanical Loading

Ferroelectrics are a widely used class of functional materials, which mostly perform simutaneously ferroelectric and ferroelastic properties. High stress can therefore effectively alter their electrical properties through the stress-induced domain evolution or phase transformation. As shown in **Figure 1**, a stress-induced insulating-to-conductive domain structure evolution in an individual $BaTiO_3$ nanopillar has been revealed via in situ TEM observation. The pillar originally displays a herringbone domain structure, which can change into a common (head-to-tail) 180°domain structure under axial tension or a head-to-head charged 180° domain structure under axial compression.[73] The strongly charged head-to-head 180° domain wall presents in fact a free-electron gas structure, exhibiting metallic-type conductivity that is 10^9 times higher than the parent $BaTiO_3$ crystal.[74,75] But it is unstable at

Yu Deng is an associate Professor at Nanjing University in the Solid State Microstructure National Key Lab and Collaborative Innovation Center of Advanced Microstructures. His research areas are electron microscopy and microanalysis of both functional and structural materials.

Ruopeng Zhang is currently a Ph.D. candidate working at both the National Center for Electron Microscopy, Molecular Foundry, Lawrence Berkeley National Laboratory and the Department of Materials Science & Engineering, University of California, Berkeley. His research interests include direct TEM observations of SRO in structural alloys, in situ TEM nanomechanical testing of stress-induced phase transformations, and method development of 4D-data analysis on both 4D-STEM and EBSD experiments.

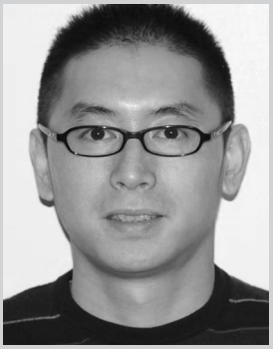

Zhiqiang Chen is a Professor at Center for High Pressure Science & Technology Advanced Research (HPSTAR) where he is the Technical Director of HPSTAR Shanghai Laboratory. His research areas mainly include crystallography, nanomaterials, functional materials, and synchrotron technology.

 © 2019 WILEY-VCH Verlag GmbH & Co. KGaA, Weinheim

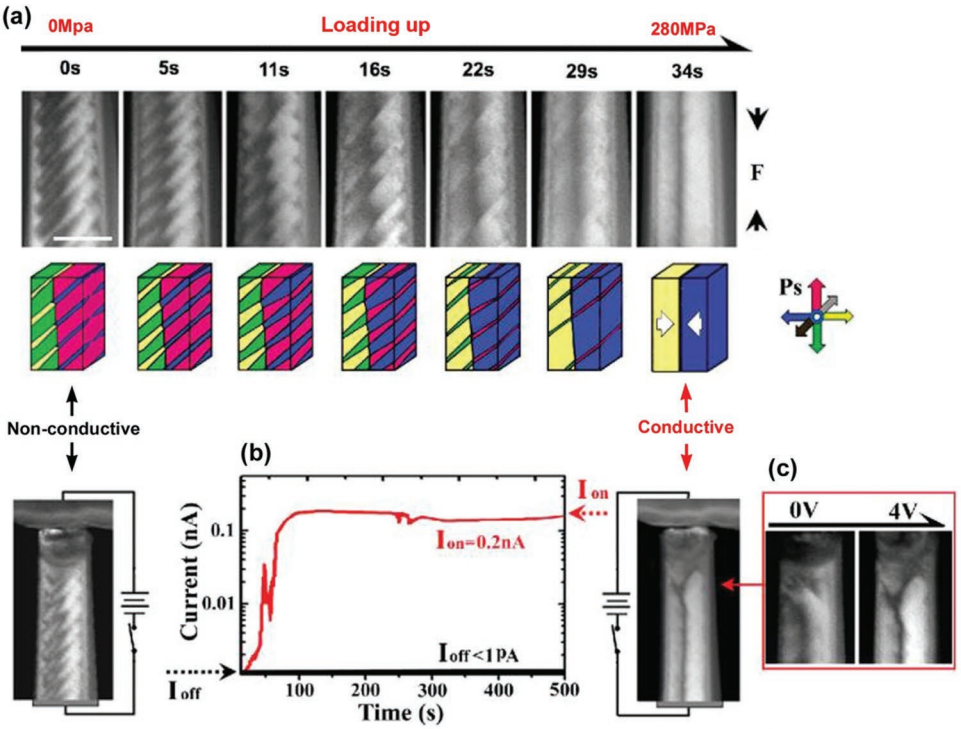

Figure 1. a) The domain evolutions in a single-crystal $BaTiO_3$ nanopillar under quantitative compression loading: from a herringbone domain structure to a charged head-to-head 180° domain structure. b) The dramatically enhanced conductivity related to the domain structure changing, i.e., the conductivity induced by a free-electron gas structure. c) The head-to-head 180° domain wall has not reached to the pillar-top electrodes, until a 4 V electric field between the top and bottom electrodes has been applied. The scale bar in (a) is 100 nm.

the natural status due to its higher energy.[74] Here the structure is formed while the compression load reaches 280 MPa (Figure 1a). A steady conductivity between the pillar substrate and the boron-doped nanoindentation tip has been detected (Figure 1b). Notably, we found that the stress-induced charged head-to-head domain wall (i.e., the free-electron gas structure) was not through the entire nanopillar at first, however showing a "deflecting growth" which avoids approaching the top electrode of the pillar, until a 4 V voltage has been applied (Figure 1c). The behavior is theoretically predicted (it needs to overcome a barrier before the head-to-head domain wall connecting the electrodes and subsequently enabling current),[74] but rarely reported via direct experimental observation. It is worth mentioned that unlike heterogeneous interfaces, domain walls in ferroelectrics can be created, displaced, annihilated and recreated, therefore triggering the reversible tuning of the functional properties through mechanical ways.

An ongoing pursuit of mechanical in situ TEM experimental systems is the integration of multifield measurement during the loading process. Examples are the application and the measurement of electrical[70,72] and thermal[34,51] properties, while applying a mechanical load on the sample. Here, precision electrical detection system, e.g., a four-point-contacting one, can be installed in the nanoindentation TEM holder. The diamond nanoindentation tip (doped with boron for good conductivity) and the TEM sample grid (made of metal) can service as top and bottom electrodes of the sample, as the mechanical loading is being performed. In addition, controllable thermal loading is available via electrical heating or electron-beam heating, as the electrical actuator or thermal expansion effect introducing the stress loading. The measured properties, direct observations, and quantitative loadings are therefore corresponding, providing critical evidences for mechanism studies.

2.2. High-Throughput In Situ 4D-STEM

4D-STEM (i.e., a nanobeam electron diffraction mapping) combines a high spatial resolution (≈1 nm) with a large field of view (≈1 µm).[76–79] To acquire a 4D-STEM dataset, one need to work in the STEM mode, where the electron probe scan through the interested area and the diffraction pattern can be recorded at each scanning position. Namely 4D-STEM dataset outputs 2D real space and 2D reciprocal-space information simultaneously, resulting in a 4D form.[78] Therefore, one data acquisition could be used for virtual-aperture diffraction contrast bright-field/dark-field (BF/DF) imaging,[39] orientation mapping,[80] large-field-of-view strain mapping,[78] and even ordering mapping.[81] The operating principle of 4D-STEM is demonstrated in **Figure 2**a along with an experimental example of a $SrTiO_3$/$PbTiO_3$ multilayer heterojunction by a multiple-channel acquisition on composition, strain, and polarization mapping.[82] Here, combining nanobeam electron diffraction mapping with in situ mechanical TEM observation allows extraction of multichannel information. The 4D-STEM application has

© 2019 WILEY-VCH Verlag GmbH & Co. KGaA, Weinheim

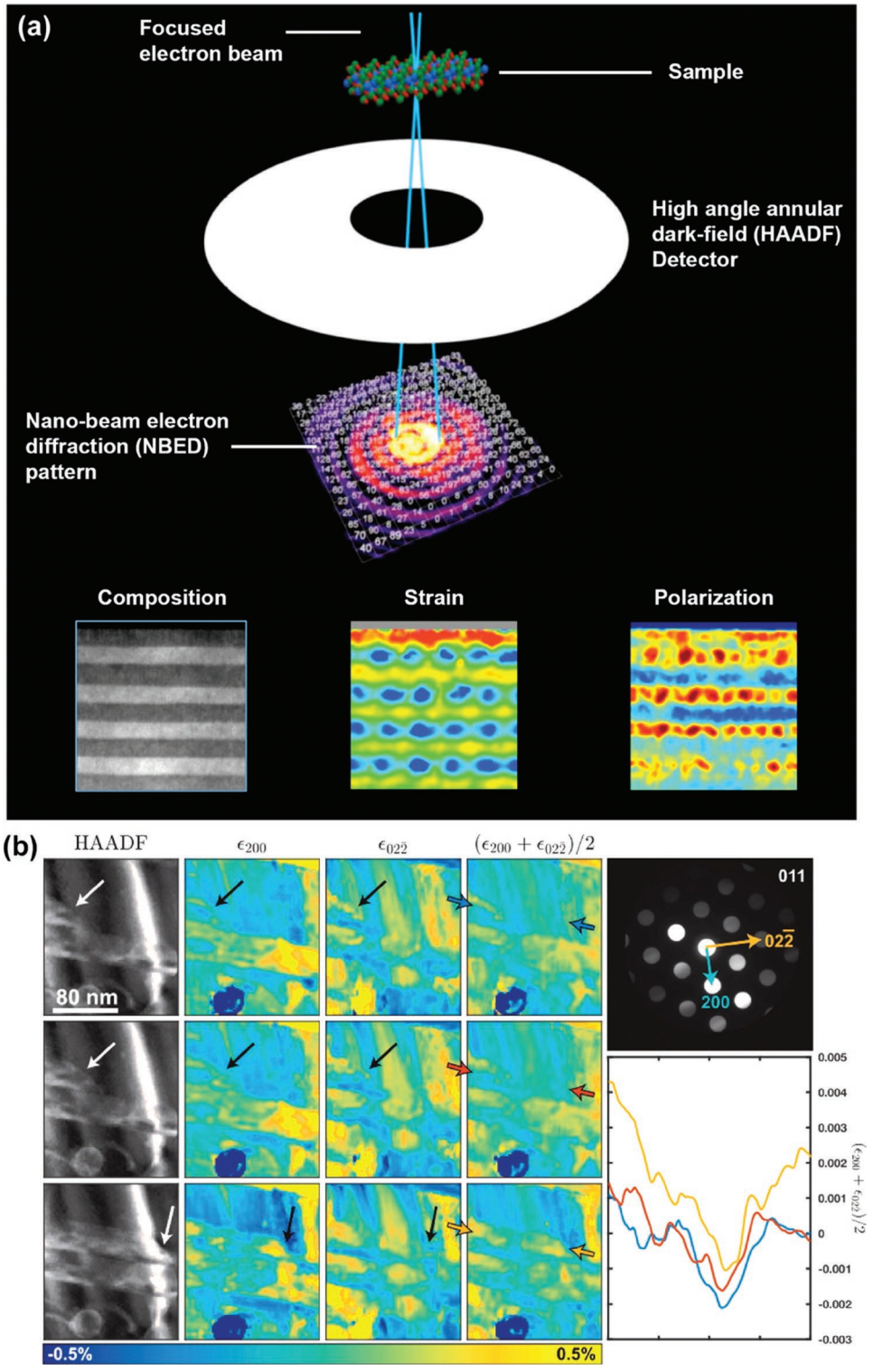

Figure 2. The in situ probing by high-throughput 4D-STEM. a) The principle of the high-throughput multichannel 4D-STEM mapping, with a case of a $SrTiO_3/PbTiO_3$ multilayer heterojunction structure. Reproduced with permission.[82] Copyright 2016, Microscopy Society of America. b) Another case of a planar slip event in structural and functional materials of stainless steel, probed in situ by 4D-STEM. Reproduced with permission.[84] Copyright 2017, Elsevier. Published by Elsevier Ltd on behalf of Acta Materialia Inc.

been significantly improved recently attributing to the deployment of fast DDD camera with frame rate up to ≈1000 fps level (at its highest pixels).[76,77,83] The fast readout speed induces a tremendous impact on high-throughput in situ STEM/TEM studies.[78,82,84,85] However, there are still challenges on large field-of-view and high resolution (e.g., unit cell scale) strain

© 2019 WILEY-VCH Verlag GmbH & Co. KGaA, Weinheim

maps for the in situ mechanical TEM, owing to such as sample drifting, sample bending, and scan noise. Many efforts are kept focusing on the field, for further technology breakthrough.

Figure 2b further exhibits an application of mechanical in situ 4D-STEM experiments on stainless steel (a structural and functional material). Pekin et al.[84] mapped the transient strains in the process of a dislocation slip event. It is found that the leading dislocation of a planar slip moves from the left to the right and the strain in the (200) direction increases behind it. However, strain in the perpendicular (02-2) direction remains unchanged, showing clear directionality when it comes to the lattice expansion. The color-coded line profiles from between the arrows in the expansion maps are also shown. Pekin et al.[85] developed a 4D-STEM method to probe the evolution of local structural ordering in the amorphous metallic glass and find the origin of the formation of shear bands.

In the near future, it is believable that the mechanical in situ 4D-STEM technique can be prominently enhanced, owing to the rapid development of high-speed DDD camera and the big data retreatment hardware/software (e.g., the machine learning). Besides local strains and the "common" microstructures such as dislocation, phase boundary and domain, the sensitive in situ 4D-STEM (equipped with energy filter and special designed apertures) is also capable to explore the local chemical short-range ordering structure and oxygen vacancy distribution. Much more robust data analysis will certainly promote the functional materials investigation.

2.3. In Situ Atomic-Resolution Observation under High Stress Loading

One recent trend of utilizing mechanical in situ STEM/TEM system is to approach extremely high stress to introduce as many microstructure evolutions as possible. Comparing with tensile load, compression and shearing load can provide much higher stress (without triggering catastrophically sample cracking, which terminates the experiment).[86] So far, high stress up to 1 GPa level is achievable in mechanical in situ STEM/TEM, mostly through shearing way (i.e., the extremely high stress is achieved locally). For most materials of interest, 1 GPa level stress is enough to trigger most microstructure evolutions including domain evolution, strain-driven phase transition, and defect nucleation.[86–88] Certainly, we need to measure the highly inhomogeneous local strain/stress distribution, since the simply measured average values cannot support the quantitative analysis. The novel 4D-STEM technique mentioned above allows us to depict the local strain at unit-cell resolution.[76–78] More, the growing availability of aberration corrected STEM/TEM[4,35] has promoted the in situ mechanical study at atomic resolution. Therefore, the atomic resolution in situ investigation of functional materials subjected to ultrahigh stress is attracting more and more research interests in recent years.

Figure 3a shows an in situ HRTEM study on a stress-induced amorphization process in crystalline silicon[89] where

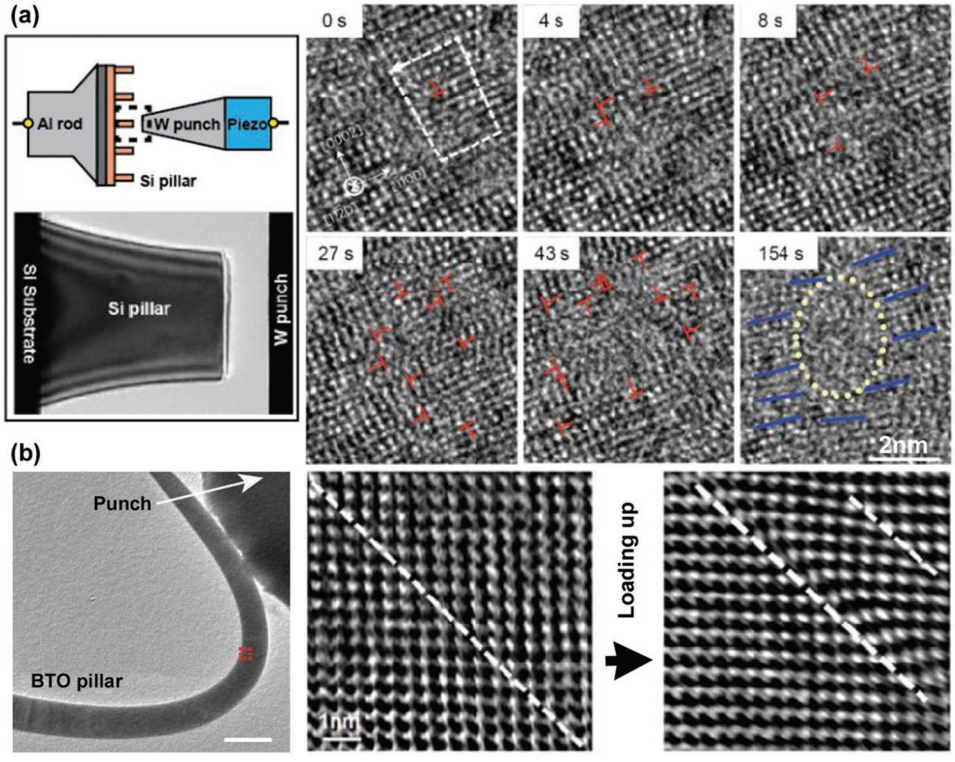

Figure 3. In situ atomic-resolution observations on dislocation nucleation under high stress loading. a) In situ TEM setup and observation of dislocation nucleation under heavy shearing (≈6 Pa), which leads to amorphization in single-crystal silicon. Reproduced with permission.[89] Copyright 2016, Springer Nature. b) The dislocation nucleation at a 90° domain wall in single-crystal $BaTiO_3$ nanopillar under high shearing (≈2 GPa), which however leads to cracking. Here, we highlight the sharp 90° domain wall with a single white dot line, and the broadened domain wall under heavy shearing with two white dot lines, respectively. Reproduced with permission.[91] Copyright 2019, Acta Materialia Inc. Published by Elsevier Ltd.

© 2019 WILEY-VCH Verlag GmbH & Co. KGaA, Weinheim

a 6 GPa shear stress has been gradually loaded on the single-crystalline Si sample, introducing large number of dislocations and eventually leading to full amorphization.[89,90] With real-time atomic-resolution observation, the dislocation nucleation, the local lattice disrupting, and amorphous Si nanodomain have been observed, clearly revealing the deformation and crystal-amorphous transformation mechanism. Figure 3b presents another in situ atomic resolution observation of crystalline $BaTiO_3$ nanopillar under the similar slow large shearing load. It is found that dislocation nucleated in the $BaTiO_3$ nanopillar at a 90° domain wall, as the local shearing stress goes up to ≈2 GPa. However, the dislocation nucleation triggered a catastrophic cracking along the domain wall, leading to a completely different result comparing with the above Si case. The various dislocation growth mechanism in $BaTiO_3$ is explained as follows:[91] 1) For stress releasing, the 90° domain wall is easily induced in $BaTiO_3$ (as the stress reaches 10 MPa level). 2) Mobile point defects (mainly oxygen vacancy in $BaTiO_3$[14]) then accumulate at the domain walls, providing the dislocation nucleation sites.[14,31,32] 3) As the stress further increased to ≈2 GPa, more and more dislocations nucleate at 90° domain wall, subsequently triggering the cracking along the domain wall.[73,91] With the atomic resolution direct observation, many critical evidences have been revealed through the mechanical in situ STEM/TEM probing, which will greatly promote the deformation mechanism study and enrich our understanding of materials science under extreme condition.

2.4. MEMS-Based In Situ Mechanical TEM

To prompt the in situ STEM/TEM probing under high-stress load and multiple-load including high-stress one, one promising way is the application of the MEMS chips, which can well stabilize sample on good zone axis, limit sample vibration amplitude, and add multiple fields simultaneously in situ, while performing the atomic-resolution observation.[92–96] For example, **Figure 4**a displays a simple passive PtP device, consisting of a θ-shaped Si frame.[51,97] The local phase transition of the VO_2 nanowire under heating has been probed by electron diffraction and dark-field observation (Figure 4b). Owing to volume change caused by the phase transition, there are corresponding strain and stress generated inside the sample. By using the PtP device, the respond speed and the stress output have been measured in situ (Figure 4c), evidently proving that the nanowire sample in fact has a potential application for actuator.

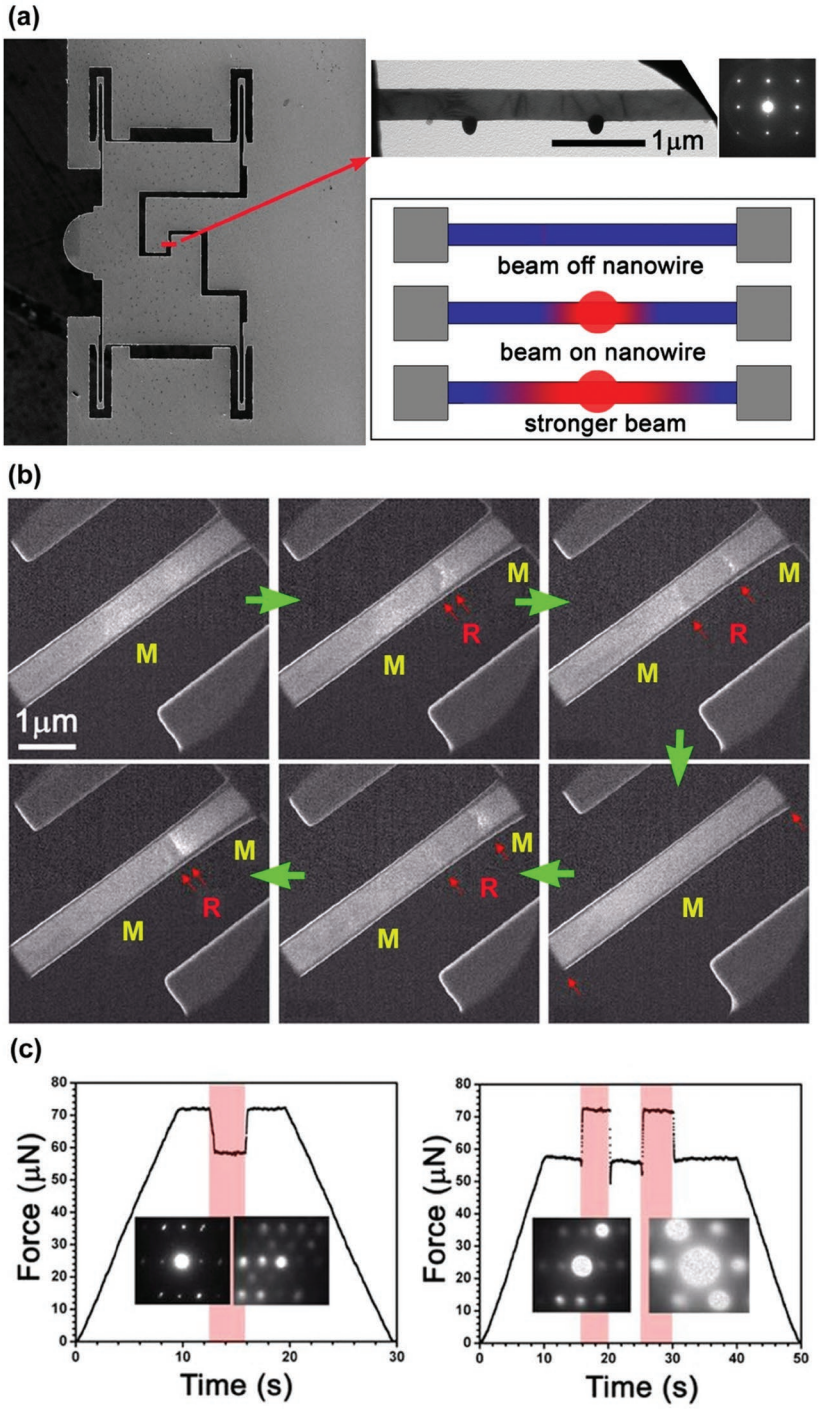

Figure 4. The strain and force output of a VO_2 nanowire under electron beam heating, being measured in situ by using a MEMS PtP chip. a) The PtP device and the VO_2 nanowire on it. The local phase transformation under heating causes a strain and force output, which can be well detected by the in situ mechanical TEM system with PtP device. b) The in situ dark-field observations of the nanowire, displaying local phase transition during a heating-and-cooling process. c) The force output depending on the local phase transformation. a) Adapted with permission.[51] Copyright 2013, AIP Publishing LLC. b,c) Reproduced with permission.[51] Copyright 2013, AIP Publishing LLC.

© 2019 WILEY-VCH Verlag GmbH & Co. KGaA, Weinheim

Recently, more and more different kinds of chips (i.e., testing platforms) which can be mounted on the sample stage of in situ TEM holder, including the e-PtP (with simultaneous electrical and mechanical systems),[93–95] and the in situ TEM tensile device based on a thermally actuated bimetallic strips,[34] have been developed. As known, the pole piece of TEM is typically no more than a few millimeters, seriously limiting the space for installing in situ equipment. Therefore the highly integrated chip device will be a solution for the next-generation mechanical in situ TEM/STEM technique, which means more functions, lower cost, and easier control.

2.5. 3D Observation in In Situ Mechanical TEM

Direct observation of defect motion and microstructure evolution under stress loading is critical for understanding the deformation mechanism of functional materials. Oftentimes, a 2D projection is not enough, since there are always complex microstructures evolutions under high stress, such as hierarchical domain/phase structures and dislocation/planer-defect which in fact interact with each other.[27,46] For example, **Figure 5**b shows a 3D self-similar nested bundle domain structure[25] in a $BaTiO_3$ micropillar under compression. It is in fact a hierarchical twinned architecture which is very efficient in releasing high stress,[91] displaying a "merged-bundle" front view and a "displaced-bundle" side view.[29] Here, simple 3D observation (i.e., taking "front" and "side" observations under the exact compression loading, respectively) can be well performed now. As in Figure 5a,c, we simply investigated a twinning domain evolution in a $BaTiO_3$ pillar under compression in 3D. However, through the strictly professional tomography way[63,98,99] it is still challenging to conduct mechanical in situ study. Now the in situ mechanical TEM holder still means a limited rotation range and a not-so-precision 3D tilting, as well as a not-so-stable sample. Nevertheless, under high stress the 3D defect motion and microstructure evolution in functional materials remains to be an attractive topic. Recently more and more efforts have been made on tomography techniques.[63] In near future, such efforts can significantly impose our understanding of functional materials under high stress.

2.6. In Situ Functional Micro-/Nanodevice Testing under Service Condition

The trend of "ultrasmall device with ultralow energy consumption" makes many integrated devices becoming increasingly miniaturized, down to sub-micrometer or even nanometer size.[93,100,101] To directly "see" their performances or find the failure mechanism of the ultrasmall devices (beyond the resolution range of optical microscope) under service condition, in situ mechanical SEM/TEM testing platforms (with multiple-field functions including the stress one) are used in more industrial fields.[93,102] They can simultaneously detect the functional properties (as mentioned above in 2.1 and 2.4) and measure the strain/stress responses. Notably, the developing of automatic control now allows us to perform complex testing such as cycling and aging by very simple programming.

Figure 6a describes the cycling test of a vanadium dioxide nanowire-based thermometer, which monitors electron beam heating effect.[97] Its very reliable metal–insulator transition

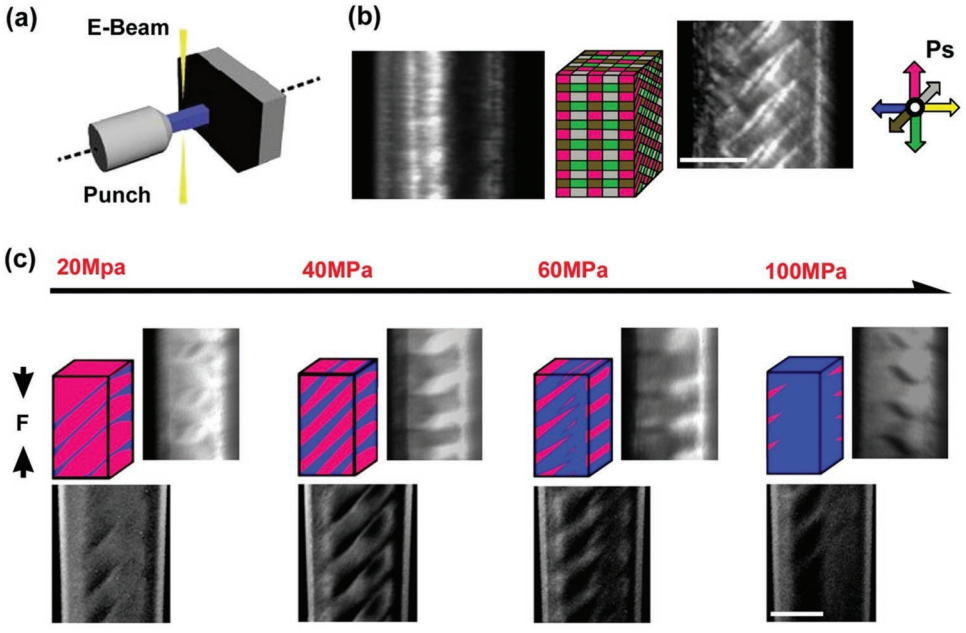

Figure 5. Simple 3D in situ observations of a $BaTiO_3$ single-crystal nanopillar under stress loading. a) Setup of the in situ mechanical TEM system. b) 3D observation of a $BaTiO_3$ nanopillar with self-similar nested bundle domain structure, being induced by cycling compression. c) 3D in situ observation of a simple twinning domain evolution in a $BaTiO_3$ nanopillar, under a compression. The scale bars in (a) and (b) are both 100 nm. The two SEM images in (b) and the three right most "front-view" TEM images in (c): Reproduced with permission.[91] Copyright 2019, Acta Materialia Inc. Published by Elsevier Ltd.

© 2019 WILEY-VCH Verlag GmbH & Co. KGaA, Weinheim

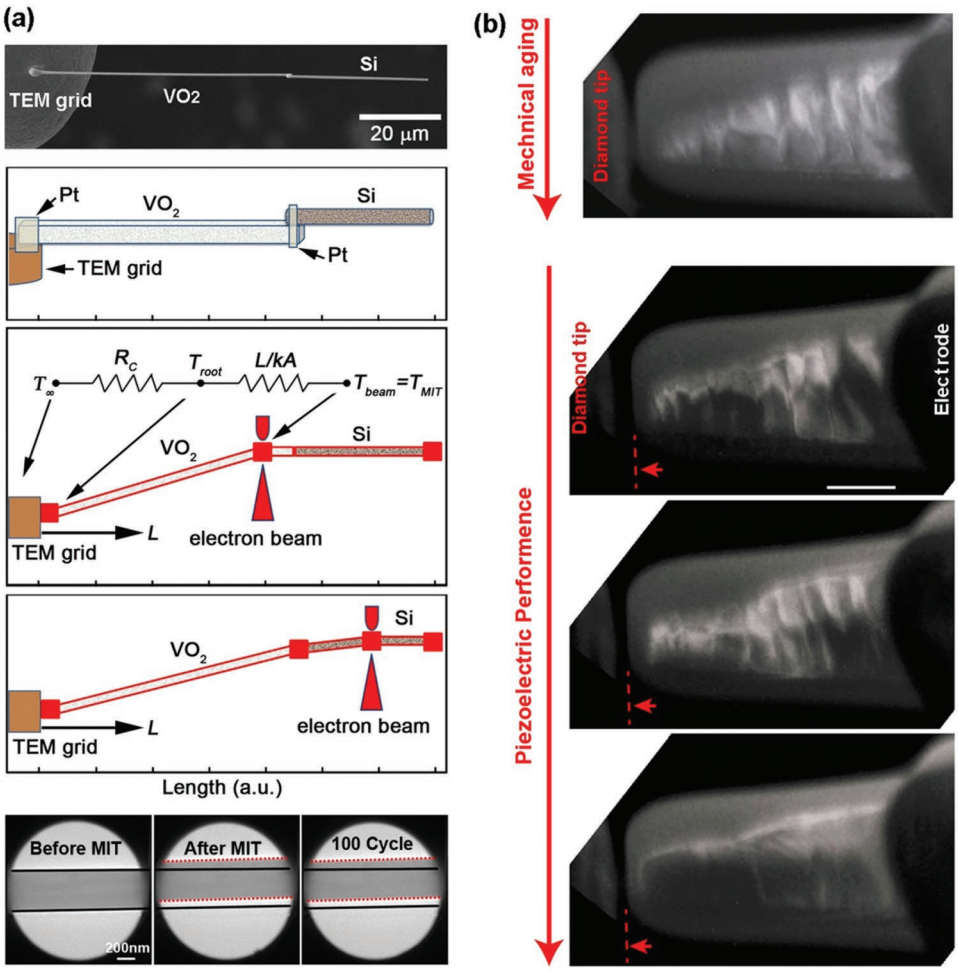

Figure 6. a) A VO_2-nanowire-based nano-thermometer which can quantitatively evaluate the temperature increasing by electron beam local heating. Its setup (by SEM observation, see upper inset), working principle (see middle three insets), and in situ TEM observation of the strain outputs under electron beam heating/cooling cycling (before and after MIT for the first cycle, and after MIT for the 100th cycle. See three lower insets). Adapted with permission.[97] Copyright 2014, Springer Nature. (The image for "100 Cycle" is a new image). b) The in situ observation of a $BaTiO_3$ nanopillar under a mechanical aging (i.e., under a compression for 100 min. See upper inset.) and the piezoelectric performance of the $BaTiO_3$ pillar (the electric field is applied between the diamond tip and bottom electrode. See three lower insets.) after the aging. The scale bar is 100 nm.

(MIT) temperature (68 °C) and precision strain output are crucial for the quantitative evaluation. The in situ testing for 100 heating/cooling cycles (by allowing/blocking beam) ensure the reliability of the device. More, Figure 6b shows a multiple-domain-structured $BaTiO_3$ nanopillar, which can work as a piezoelectric actuator. Interestingly, it shows an enhanced strain output after a mechanical aging. Here, many nano-domains have been introduced into the nanopillar under compression load and then stabilized by a time-dependent point defect pinning effect,[10,33,91] resulting in a typical "domain engineering" effect[12,13] which improves the piezoelectric property.

Thanks to the recent development of environmental in situ TEM techniques, more service conditions can be applied (e.g., the gas environment for hydrogen embrittlement study) simultaneously with external fields.[93] For the service-condition testing, the in situ mechanical SEM/TEM system provides great opportunity, since it can work as both actuator and detector.

3. Summary and Prospects

We have highlighted the recent progress of in situ mechanical SEM/TEM for functional materials study. Now we can directly observe and multiple-channel measure the local domain evolution and phase transition, as well as defect motions, which are critical for understanding the materials property changing under high stress. We believe that the combination using of multiple fields in situ, such as the mechanical, electrical and thermal ones, as well as the programmed automatically testing, can pave the road in functional materials researches.

An important trend of utilizing mechanical in situ SEM/TEM is to combine experimental approach with novel atomistic simulation. There are extensive reports that deployed this strategy. Instead of elaborating all, several representative cases have been raised here. Sun et al.[103] conducted in situ TEM compression experiments and reported a theoretically predicted liquid-like metal nanoparticles. They observed atomic

© 2019 WILEY-VCH Verlag GmbH & Co. KGaA, Weinheim

layer growth during compression, which can be explained by a surface-diffusion-dominated Coble mechanism. Molecular dynamics (MD) simulations corroborated such a process by providing the detailed mass transportation route. The same methodology can also be widely applied to study other material systems. Yu et al.[102] conducted in situ TEM nanopillar compression experiments on Ti-O alloys with varying oxygen content (Ti-0.1 wt% O, Ti-0.2 wt% O, and Ti-0.3 wt% O) and observed a potent hardening effect with increasing oxygen content, which cannot be fully explained by elasticity theory. First-principles calculations revealed that during the dislocation slip event, the oxygen atom would experience a "mechanical shuffle" among different interstitial sites. This strong interaction provided a strong pinning effect of dislocation motions.

In the near future, we believe that in situ mechanical SEM/TEM methods would continue to further evolve in the many aspects: 1) Incorporation with more in situ capabilities such as magnetic field control and measurement, laser pump-probe, and environmental atmosphere, etc. 2) Improved temporal resolution with the development of faster electron detector and novel dynamic TEM techniques. 3) Strong and standardized data analysis tools (with the machine learning software[104,105]) to work with high-throughput raw data associated with high spatial/temporal resolution or information-rich characterizations such as 4D-STEM.

Acknowledgements

Y.D., R.Z., and Z.C. contributed equally to this work. The authors acknowledge support by the National Natural Science Foundation of China (Grants No. 50802039) and Natural Science Foundation of Jiangsu Province, China (Grant No. BK20151382) and National Natural Science Foundation of China (Grant No. U1530402 and No. U1732120). A.M. acknowledges support from the National Science Foundation through the STROBE Science and Technology Center. R.Z. acknowledges funding from the US Office of Naval Research under Grant No. N00014-12-1-0413. T.P. was funded by the U.S. Department of Energy, Office of Science, Office of Basic Energy Sciences, Materials Sciences, and Engineering Division under Contract No. DE-AC02-05-CH11231 within the Mechanical Behavior of Materials program (KC13). J.C. and C.O. acknowledge additional support from the Department of Energy Early Career Research Program. S.Z. acknowledges funding from the US Office of Naval Research under Grant No. N00014-17-1-2283. The electron microscopy work was performed at the Molecular Foundry, Lawrence Berkeley National Laboratory, which is supported by the U.S. Dept. of Energy under Contract # DE-AC02-05CH11231.

Conflict of Interest

The authors declare no conflict of interest.

Keywords

4D-STEM, functional materials, in situ, microstructures, transmission electron microscopy

Received: September 17, 2019
Revised: October 7, 2019
Published online:

[1] E. A. Stach, *Mater. Today* **2008**, *11*, 50.
[2] H. Liao, L. Cui, S. Whitelam, H. Zheng, *Science* **2012**, *336*, 1011.
[3] R. M. van der Veen, O.-H. Kwon, A. Tissot, A. Hauser, A. H. Zewail, *Nat. Chem.* **2013**, *5*, 395.
[4] M. L. Taheri, E. A. Stach, I. Arslan, P. A. Crozier, B. C. Kabius, T. LaGrange, A. M. Minor, S. Takeda, M. Tanase, J. B. Wanger, R. Sharma, *Ultramicroscopy* **2016**, *170*, 86.
[5] R. Sharma, *Micron* **2012**, *43*, 1147.
[6] E. Spiecker, S. H. Oh, Z. Shan, Y. Ikuhara, S. Mao, *MRS Bull.* **2019**, *44*, 443.
[7] Z. L. Wang, *Adv. Mater.* **2003**, *15*, 1497.
[8] T. T. A. Lummen, Y. Gu, J. Wang, S. Lei, F. Xue, A. Kumar, A. T. Barnes, E. Barnes, S. Denev, A. Belianinov, M. Holt, A. N. Morozovska, S. V. Kalinin, L.-Q. Chen, V. Gopalan, *Nat. Commun.* **2014**, *5*, 3172.
[9] L. Kong, G. Liu, W. Yang, W. Cao, *Appl. Phys. Lett.* **2015**, *107*, 042901.
[10] X. Ren, *Nat. Mater.* **2004**, *3*, 91.
[11] S. Tsukada, T. H. Kim, S Kojima, *APL Mater.* **2013**, *1*, 032114.
[12] S. Wada, H. Kakemoto, T. Tsurumi, *Mater. Trans.* **2004**, *45*, 178.
[13] S. Wada, T. Muraishi, K. Yokoh, K. Yako, H. Kamemoto, T. Tsurumi, *Ferroelectrics* **2007**, *355*, 37.
[14] J. C. Agar, A. R. Damodaran, M. B. Okatan, J. Kacher, C. Gammer, R. K. Vasudevan, S. Pandya, L. R. Dedon, R. V. K. Mangalam, G. A. Velarde, S. Jesse, N. Balke, A. M. Minor, S. V. Kalinin, L. W. Martin, *Nat. Mater.* **2016**, *15*, 549.
[15] Q. Yang, J. X. Cao, Y. C. Zhou, Y. Zhang, Y. Ma, X. J. Lou, *Appl. Phys. Lett.* **2013**, *103*, 142911.
[16] Y. W. Li, X. B. Ren, F. X. Li, H. S. Luo, D. N. Fang, *Appl. Phys. Lett.* **2013**, *102*, 092905.
[17] J. Paul, T. Nishimatsu, Y. Kawazoe, U. V. Waghmare, *Phys. Rev. B* **2009**, *80*, 024107.
[18] F. Ke, H. Dong, Y. Chen, J. Zhang, C. Liu, J. Zhang, Y. Gan, Y. Han, Z. Chen, C. Gao, J. Wen, W. Yang, X.-J. Chen, V. Struzhkin, H.-K. Mao, B. Chen, *Adv. Mater.* **2017**, *29*, 1701983.
[19] J Schiftz, K. W. Jacobsen, *Science* **2003**, *301*, 1357.
[20] P. P. Edwards, F. Hensel, *Nature* **1997**, *388*, 621.
[21] G. Catalan, J. Seidel, R. Ramesh, J. F. Scott, *Rev. Mod. Phys.* **2012**, *84*, 119.
[22] J. F. Scott, *Science* **2007**, *315*, 954.
[23] H. Lu, C.-W. Bark, D. Esqué-de los Ojos, J. Alcala, C. B. Eom, G. Catalan, A. Gruverman, *Science* **2012**, *336*, 59.
[24] R. J. Zeches, M. D. Rossell, J. X. Zhang, A. J. Hatt, Q. He, C.-H. Yang, A. Kumar, C. H. Wang, A. Melville, C. Adamo, G. Sheng, Y.-H. Chu, J. F. Ihlefeld, R. Erni, C. Ederer, V. Gopalan, L. Q. Chen, D. G. Schlom, N. A. Spaldin, L. W. Martin, R. Ramesh, *Science* **2009**, *326*, 977.
[25] L.-W. Chang, V. Nagarajan, J. F. Scott, J. M. Gregg, *Nano Lett.* **2013**, *13*, 2553.
[26] Y. M. Jin, Y. U. Wang, A. G. Khachaturyan, *J. Appl. Phys.* **2003**, *94*, 3629.
[27] Z. W. Shan, G. Adesso, A. Cabot, M. P. Sherburne, S. A. Syed Asif, O. L. Warren, D. C. Chrzan, A. M. Minor, A. P. Alivisatos, *Nat. Mater.* **2008**, *7*, 947.
[28] T. Asada, Y. Koyama, *Phys. Rev. B* **2007**, *75*, 214111.
[29] Y. Ivry, D. P. Chu, C. Durkan, *Nanotechnology* **2010**, *21*, 065702.
[30] E. A. Eliseev, A. N. Morozovska, Y. Gu, A. Y. Borisevich, L.-Q. Chen, V. Gopalan, S. V. Kalinin, *Phys. Rev. B* **2012**, *86*, 085416.
[31] I. Stolichnov, L. Feigl, L. J. McGilly, T. Sluka, X.-K. Wei, E. Colla, A. Crassous, K. Shapovalov, P. Yudin, A. K. Tagantsev, N. Setter, *Nano Lett.* **2015**, *15*, 8049.
[32] W. T. Lee, E. K. H. Salje, *Appl. Phys. Lett.* **2005**, *87*, 143110.
[33] X. Ren, Y. Wang, K. Otsuka, P. Lloveras, T. Castán, M. Porta, A. Planes, A. Saxena, *MRS Bull.* **2009**, *34*, 838.
[34] L. Wang, J. Teng, X. Sha, J Zou, Z. Zhang, X. Han, *Nano Lett.* **2017**, *17*, 4733.

 © 2019 WILEY-VCH Verlag GmbH & Co. KGaA, Weinheim

[35] P. Liu, X. Wei, S. Song, L. Wang, A. Hirata, T. Fujita, X. Han, Z. Zhang, M. Chen, *Acta Mater.* **2019**, *165*, 99.
[36] A. M. Minor, S. A. S. Asif, Z. Shan, E. A. Stach, E. Cyrankowski, T. J. Wyrobek, O. L. Warren, *Nat. Mater.* **2006**, *5*, 697.
[37] R. Ramachandramoorthy, R. Bernal, H. D. Espinosa, *ACS Nano* **2015**, *9*, 4675.
[38] V. Samaee, R. Gatti, B. Devincre, T. Pardoen, D. Schryvers, H. Idrissi, *Sci. Rep.* **2018**, *8*, 12012.
[39] C. Gammer, V. B. Ozdol, C. H. Liebscher, A. M. Minor, *Ultramicroscopy* **2015**, *155*, 1.
[40] C.-H. Chiu, C.-W. Huang, Y.-H. Hsieh, J.-Y. Chen, C.-F. Chang, Y.-H. Chu, W.-W. Wu, *Nano Energy* **2017**, *34*, 103.
[41] C. Chisholm, H. Bei, M. B. Lowry, J. Oh, S. A. Syed Asif, O. L. Warrren, Z. W. Shan, E. P. George, A. M. Minor, *Acta Mater.* **2012**, *60*, 2258.
[42] C. T. Nelson, P Gao, J. R. Jokisaari, C. Heikes, C. Adamo, A. Melville, S.-H. Baek, C. M. Folkman, B. Winchester, Y. Gu, Y. Liu, K. Zhang, E. Wang, J. Li, L.-Q. Chen, C.-B. Eom, D. G. Schlom, X. Pan, *Science* **2011**, *334*, 968.
[43] D. A. Muller, N. Nakagawa, A. Ohtomo, J. L. Grazul, H. Y. Hwang, *Nature* **2004**, *430*, 657.
[44] S. H. Oh, M. Legros, D Kiener, G. Dehm, *Nat. Mater.* **2009**, *8*, 95.
[45] K. S. Ng, A. H. W. Ngan, *Acta Mater.* **2009**, *57*, 4902.
[46] Q. Yu, M. Legros, A. M. Minor, *MRS Bull.* **2015**, *40*, 62.
[47] R. P. Sankaran, V. B. Ozdol, C. Ophus, J. Kacher, C. Gammer, S. Govindjee, A. M. Minor, J. W. Morris Jr., *Acta Mater.* **2018**, *151*, 334.
[48] C. Ophus, *Adv. Struct. Chem. Imaging* **2017**, *3*, 13.
[49] Z. Liu, M. A. Monclús, L. W. Yang, M. Castillo-Rodríguez, J. M. Molina-Aldareguía, J. LLorca, *Extreme Mech. Lett.* **2018**, *25*, 60.
[50] Y. Yang, Z. Fu, X. Zhang, Y. Cui, F. Xu, T. Yue, L. Wang, *Ultramicroscopy* **2019**, *198*, 43.
[51] H. Guo, K. Wang, Y. Deng, Y. Oh, S. A. Syed Asif, O. L. Warren, Z. W. Shan, J. Wu, A. M. Minor, *Appl. Phys. Lett.* **2013**, *102*, 231909.
[52] M. D. Uchic, P. A. Shade, D. M. Dimiduk, *JOM* **2009**, *61*, 36.
[53] J. H. Han, M. T. A. Saif, *Rev. Sci. Instrum.* **2006**, *77*, 045102.
[54] H. G. F. Wilsdorf, *Rev. Sci. Instrum.* **1958**, *29*, 323.
[55] D. B. Williams, C. B. Carter, *The Transmission Electron Microscope*, Springer, Boston, MA **1996**, pp. 3–22.
[56] P. B. Hirsch, R. W. Horne, M. J. Whelan, *Philos. Mag.* **1956**, *1*, 4553.
[57] J. Pelissier, P. Debrenne, *Microsc., Microanal., Microstruct.* **1993**, *4*, 111.
[58] H. Ohnishi, Y. Kondo, K. Takayanagi, *Nature* **1998**, *395*, 780.
[59] M. A. Wall, U. Dahmen, *Microsc. Res. Tech.* **1998**, *42*, 248.
[60] T. Kizuka, *Phys. Rev. B* **1998**, *57*, 11158.
[61] Z. W. Shan, R. K. Mishra, S. A. S. Asif, O. L. Warren, A. M. Minor, *Nat. Mater.* **2008**, *7*, 115.
[62] D. Kiener, A. M. Minor, *Acta Mater.* **2011**, *59*, 1328.
[63] B.-Y. Liu, F. Liu, N. Yang, X.-B. Zhai, L. Zhang, Y. Yang, B. Li, J. Li, E. Ma, J.-F. Nie, Z.-W. Shan, *Science* **2019**, *365*, 73.
[64] A. M. Minor, J. W. Morris, E. A. Stach, *Appl. Phys. Lett.* **2001**, *79*, 1625.
[65] Z. L. Wang, P. Poncharal, W. A. De Heer, *J. Phys. Chem. Solids* **2000**, *61*, 1025.
[66] W. C. Oliver, G. M. Pharr, *J. Mater. Res.* **1992**, *7*, 1564.
[67] Z. Zhang, H. Sheng, Z. Wang, B. Gludovatz, Z. Zhang, E. P. George, Q. Yu, S. X. Mao, R. O. Ritchie, *Nat. Commun.* **2017**, *8*, 14390.
[68] P. M. Voyles, J. M. Gibson, M. M. J. Treacy, *J. Electron Microsc.* **2000**, *49*, 259.
[69] P. M. Voyles, D. A. Muller, *Ultramicroscopy* **2002**, *93*, 147.
[70] J. X. Zhang, B. Xiang, Q. He, J. Seidel, R. J. Zechese, P. Yu, S. Y. Yang, C. H. Wang, Y.-H. Chu, L. W. Martin, A. M. Minor, R. Ramesh, *Nat. Nanotechnol.* **2011**, *6*, 97.
[71] Y. Yang, J. H. Jung, B. K. Yun, F. Zhang, K. C. Pradel, W. Guo, Z. L. Wang, *Adv. Mater.* **2012**, *24*, 5357.
[72] P. Gao, J. Britson, J. R. Jokisaari, C. T. Nelson, S.-H. Baek, Y. Wang, C.-B. Eom, L.-Q. Chen, X. Pan, *Nat. Commun.* **2013**, *4*, 2791.
[73] N. T. Tsou, P. R. Potnis, J. E. Huber, *Phys. Rev. B* **2011**, *83*, 184120.
[74] T. Sluka, A. K. Tagantsev, P. Bednyakov, N. Setter, *Nat. Commun.* **2013**, *4*, 1808.
[75] M. Y. Gureev, A. K. Tagantsev, N. Setter, *Phys. Rev. B* **2011**, *83*, 184104.
[76] E. A. Stach, D. Zakharov, R. D. Rivas, P. Longo, M. Lent, A. Gubbens, C. Czarnik, *Microsc. Microanal.* **2013**, *19*, 392.
[77] I. J. Johnson, K. C. Bustillo, J. Ciston, B. R. Draney, P. Ercius, E. Fong, A. Goldschmidt, J. M. Joseph, J. R. Lee, A. M. Minor, C. Ophus, A. Selvarajan, D. E. Skinner, T. Stezelberger, C. S. Tindall, P. Denes, *Microsc. Microanal.* **2018**, *24*, 166.
[78] V. B. Ozdol, C. Gammer, X. G. Jin, P. Ercius, C. Ophus, J. Ciston, A. M. Minor, *Appl. Phys. Lett.* **2015**, *106*, 253107.
[79] C. Gammer, T. C. Pekin, C. Ophus, A. M. Minor, J. Eckert, *ICTAEM 2018: Proceedings of the First International Conference on Theoretical, Applied and Experimental Mechanics*, Springer, Cham, Switzerland **2018**, pp. 356–357.
[80] O. Panova, X. C. Chen, K. C Bustillo, C. Ophus, M. P. Bhatt, N. Balsara, A. M. Minor, *Micron* **2016**, *88*, 30.
[81] R. Zhang, R. Traylor, T. Pekin, B. Ozdol, C. Ophus, A. M. Minor, *Microsc. Microanal.* **2018**, *24*, 210.
[82] J. Ciston, C. Ophus, P. Ercius, Y. Yang, R. dos Reis, C. T. Nelson, S.-L. Hsu, C. Gammer, B. V. Özdöl, Y. Deng, A. M. Minor, *Microsc. Microanal.* **2016**, *22*, 1412.
[83] A. Myasnikov, S. Zheng, D. Bulkley, Y. Cheng, D. Agard, *Microsc. Microanal.* **2018**, *24*, 890.
[84] T. C. Pekin, C. Gammer, J. Ciston, C. Ophus, A. M. Minor, *Scr. Mater.* **2018**, *146*, 87.
[85] T. C. Pekin, J. Ding, C. Gammer, B. Ozdol, C. Ophus, M. Asta, R. O. Ritchie, A. M. Minor, *Nat. Commun.* **2019**, *10*, 2445.
[86] J. Wang, S. X. Mao, *Extreme Mech. Lett.* **2016**, *8*, 127.
[87] P. Schweizer, C. Dolle, E. Spiecker, *Sci. Adv.* **2018**, *4*, eaat4712.
[88] D. C. Lupascu, Y. A. Genenko, N. Balke, *J. Am. Ceram. Soc.* **2006**, *89*, 224.
[89] Y. He, L. Zhong, F. Fan, C. Wang, T. Zhu, S. X. Mao, *Nat. Nanotechnol.* **2016**, *11*, 866.
[90] M. M. Treacy, K. B. Borisenko, *Science* **2012**, *335*, 950.
[91] Y. Deng, C. Gammer, J. Ciston, P. Ercius, C. Ophus, K. Bustillo, C. Song, R. Zhang, D. Wu, Y. Du, Z. Chen, H. Dong, A. G. Khachaturyan, A. M. Minor, *Acta Mater.* **2019**, *181*, 501.
[92] T. Sato, L. Jalabert, H. Fujita, *Microelectron. Eng.* **2013**, *112*, 269.
[93] A. M. Minor, G. Dehm, *MRS Bull.* **2019**, *44*, 438.
[94] H. D. Espinosa, R. A. Bernal, T. Filleter, *Small* **2012**, *8*, 3233.
[95] H. D. Espinosa, Y. Zhu, N. Moldovan, *J. Microelectromech. Syst.* **2007**, *16*, 1219.
[96] B. Pant, B. L. Allen, T. Zhu, K. Gall, O. N. Pierron, *Appl. Phys. Lett.* **2011**, *98*, 053506.
[97] H. Guo, M. I. Khan, C. Cheng, W. Fan, C. Dames, J. Wu, A. M. Minor, *Nat. Commun.* **2014**, *5*, 4986.
[98] K. Thompson, P. L. Flaitz, P. Ronsheim, D. J. Larson, T. F Kelly, *Science* **2007**, *317*, 1370.
[99] P. Ercius, O. Alaidi, M. J. Rames, G. Ren, *Adv. Mater.* **2015**, *27*, 5638.
[100] Z. Fan, L. Zhang, D. Baumann, L. Mei, Y. Yao, X. Duan, Y. Shi, J. Huang, Y. Huang, X. Duan, *Adv. Mater.* **2019**, *11*, 201900608.
[101] K. Bhattacharya, R. D. James, *Science* **2005**, *307*, 53.
[102] Q. Yu, L. Qi, T. Tsuru, R. Traylor, D. Rugg, J. W. Morris Jr., M. Asta, D. C. Chrzan, A. M. Minor, *Science* **2015**, *347*, 635.
[103] J. Sun, L. He, Y.-C. Lo, T. Xu, H. Bi, L. Sun, Z. Zhang, S. X. Mao, J. Li, *Nat. Mater.* **2014**, *13*, 1007.
[104] W. Li, K. G. Field, D. Morgan, *Compos. Mater.* **2018**, *36*, 4.
[105] S. Jesse, M. Chi, A. Belianinov, C. Beekman, S. V. Kalinin, A. Y. Borisevich, A. R. Lupini, *Sci. Rep.* **2016**, *6*, 26348.

© 2019 WILEY-VCH Verlag GmbH & Co. KGaA, Weinheim